

Reflection of Annual Rossby Waves at The Maritime Western Boundary of the Tropical Pacific

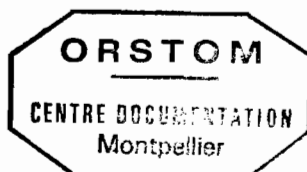
Warren B. WHITE, Nicholas GRAHAM and Chang-Kou TAI

Scripps Institution of Oceanography
Mail Code A-030
University of California at San Diego
La Jolla, California 92093, U.S.A.

Baroclinic Rossby wave activity in the tropical Pacific was first observed by White (1977), who examined the annual cycle of subsurface thermal structure in the eastern region from 10°-20°N, finding westward propagating annual signals emanating from the eastern boundary, propagating eastward at baroclinic Rossby wave speeds to the longitude of the Hawaiian Archipelago. This work was followed by Meyers (1979), who observed westward propagation of the annual cycle in upper ocean thermal structure at baroclinic Rossby wave speeds near 6°N all across the Pacific. Subsequently, White (1983) examined interannual variability in the subsurface thermal structure in the western North Pacific, finding westward propagating signals traveling at baroclinic Rossby wave speeds from 6°-30°N. These interannual waves were associated with ENSO activity. Soon thereafter, interannual baroclinic Rossby wave activity in the latitude bands from 5°-15°N and from 5°-15°S was found to act as a precursor (e.g., White et al., 1985a; Pazan et al., 1986) to the onset of the 1982-1983 El Nino activity in the eastern equatorial Pacific; indirect evidence was found that the incidence of this baroclinic Rossby wave activity in these latitude bands was instigating baroclinic Kelvin wave activity in the equatorial wave-guide. Subsequently, White et al. (1987) used this information to demonstrate that both the observation and model simulation of baroclinic Rossby wave activity in the western tropical Pacific could be used to hindcast El Nino activity in the eastern equatorial Pacific for up to a year in advance over the 25-year period from 1962-1987.

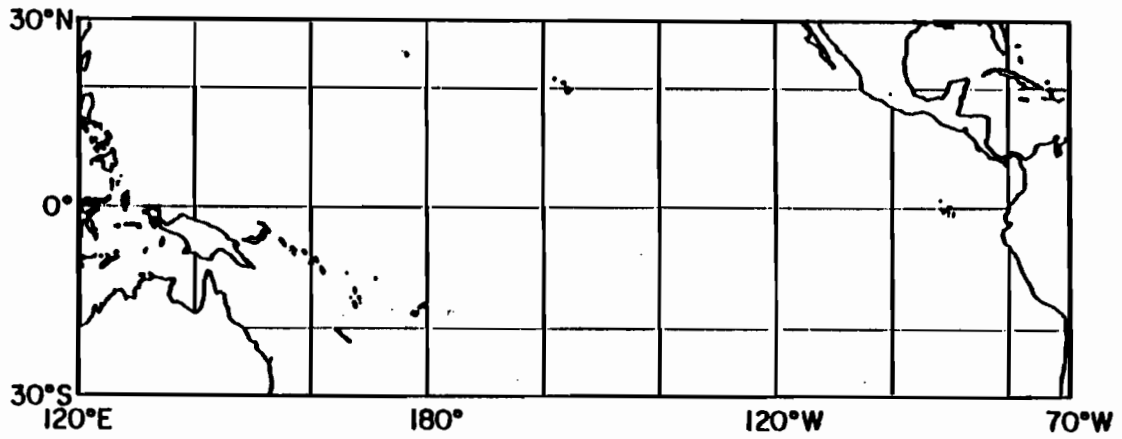
The dynamical influence that baroclinic Rossby wave activity has upon in the maintenance of the quasi-cyclic behavior of ENSO (El Nino/Southern Oscillation) was discussed by Graham and White (1988). They established using a conceptual model that baroclinic Rossby wave activity influenced ocean/atmosphere coupling in the equatorial wave-guide by providing for a steady upwelling/downwelling (lasting from 3-9 months) through the excitation of upwelling/downwelling equatorial baroclinic Kelvin wave activity at the western boundary (via the Rossby wave reflection process). During the year prior to El Nino activity in the eastern equatorial Pacific, downwelling equatorial Kelvin wave activity was associated with a steady eastward advection of warm water from the western equatorial Pacific into the central and eastern equatorial ocean, advected by the associated zonal eastward current; this eastward displacement of warm SST's on the equator was hypothesized to instigate a coupled unstable wave in the ocean/atmospheric system along the equator, of the kind discussed by Schopf and Suarez (1988). Within this conceptual model, the reflection of baroclinic Rossby waves at the western boundary of the tropical Pacific also played an important role in turning the El Nino process off, leading to La Nina, as discussed in Graham and White (1988).

Sources of baroclinic Rossby wave activity in the tropical Pacific are fairly well known. White (1977) found evidence consistent with the idea that baroclinic Rossby waves were being generated at the eastern boundary through the action of the wind stress



F30206

MAP OF THE TROPICAL PACIFIC



MAP OF THE WESTERN TROPICAL PACIFIC

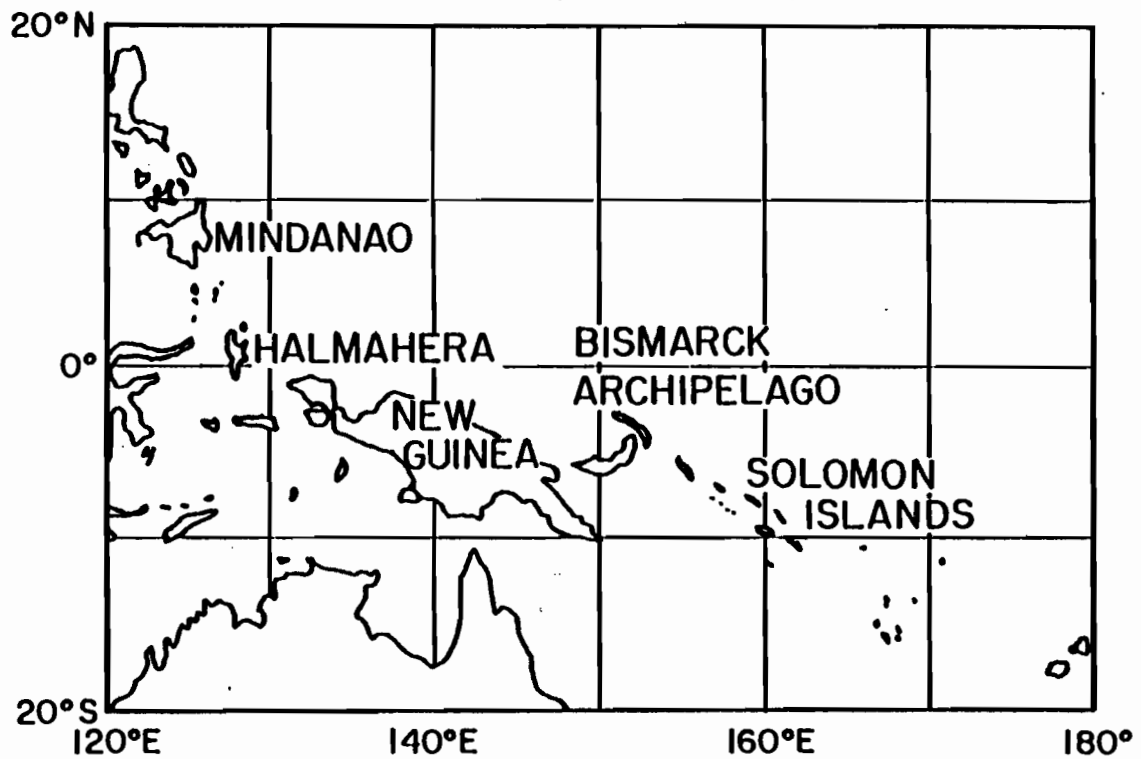


FIG.1. (Upper Panel): Map of the tropical Pacific from 30°N to 30°S where this study was conducted. (Lower Panel): Map of the western tropical Pacific, where the reflection of baroclinic Rossby waves by the maritime western boundary is emphasized.

curl. Meyers (1979) found baroclinic Rossby waves of annual period in the western and central tropical North Pacific to have been generated by the Ekman pumping in the Trade Wind field in the eastern tropical North Pacific. Later, White et al (1985b) demonstrated that the interannual baroclinic Rossby wave activity in the western North Pacific was wind-generated in response to Ekman pumping in the western and central tropical Pacific. Moreover, it was shown that baroclinic Rossby wave activity increased in amplitude toward the west in response to resonance with the wind stress curl forcing. Pazan and White (1987) computed a vorticity/volume budget for the western tropical Pacific from 4°-16°N, 160°E-160°W, finding the thermocline to have been pumped vertically in response both to the divergence of Ekman transport in the upper layer (i.e., indicative of Ekman pumping) and to the divergence of geostrophic transport in the region (i.e., indicative of Rossby wave propagation). More recently, White et al. (1989) demonstrated that it was possible to track interannual baroclinic Rossby wave activity all the way across the ocean from the eastern boundary to the western boundary in both observations and the models at approximately 12°N; regardless, Graham et al. (1989) found that most of the magnitude in this wave activity occurred in response to wind stress curl forcing in the central and western tropical Pacific, amplified by resonant forcing.

The reflection of baroclinic Rossby wave activity at the maritime western boundary of the tropical Pacific has been inferred from the statistical correlation between anomalous upper layer thickness in the off-equatorial western tropical Pacific (associated with baroclinic Rossby wave activity) and that in the central and eastern equatorial Pacific (associated with baroclinic Kelvin wave activity) in both models and observations (Pazan et al., 1986). Still, no direct observational evidence exists for the reflection of baroclinic Rossby wave activity at this western boundary and the subsequent generation of equatorial Kelvin wave activity emanating from it. A certain amount of skepticism surrounds the reflection process at the maritime western boundary (i.e., formed by the Philippines Archipelago in the northern hemisphere and possibly the Solomon Archipelago in the southern hemisphere, as shown in Fig. 1) because of the presence of gaps in the numerous archipelagoes that could conceivably constitute the maritime western boundary of the tropical Pacific. However, recently Clark (1989) and du Penhoat and Cane (1989) established that these particular archipelagoes were quite good reflectors of interannual Rossby wave activity, reflecting 70-80% of the incident baroclinic Rossby wave activity as baroclinic equatorial Kelvin waves.

In this study, the examination of GEOSAT altimetric sea level differences provides the first direct evidence of this reflection process operating at the maritime western boundary of the tropical Pacific in both the northern and southern hemisphere (see Fig.1). In an earlier study, Tai et al. (1989) analyzed altimetric sea level crossover differences from the first 17 months of the GEOSAT mission from November 1985-April 1987, finding statistically significant agreement with *in situ* measurements of sea level differences (i.e., island sea level and relative dynamic height). In that study the dominant time scale of variability that could be studied was the annual cycle; interannual variability could not be addressed because of the relatively short length of the record. So too in this study; only the wave reflection at the maritime western boundary of the tropical Pacific associated with the annual cycle is addressed.

In the earlier study of Tai et al. (1989), a time series of maps of altimetric sea level residuals in the tropical Pacific (17 months from April 23, 1985 to September 8, 1986, separated into thirty 17-day time steps) was generated. Verification of these maps was conducted by Tai et al., (1989) from the comparison of the maps of altimetric sea level residuals to similar maps of relative dynamic height (0/400 db) residuals, and time sequences of altimetric sea level residuals to similar time sequences of sea level residuals measured at island stations. Examples of these 17-day maps is given in Fig.2,

FEATURE TRACKING OF ALTIMETRIC SEA LEVEL
IN THE WESTERN NORTH PACIFIC

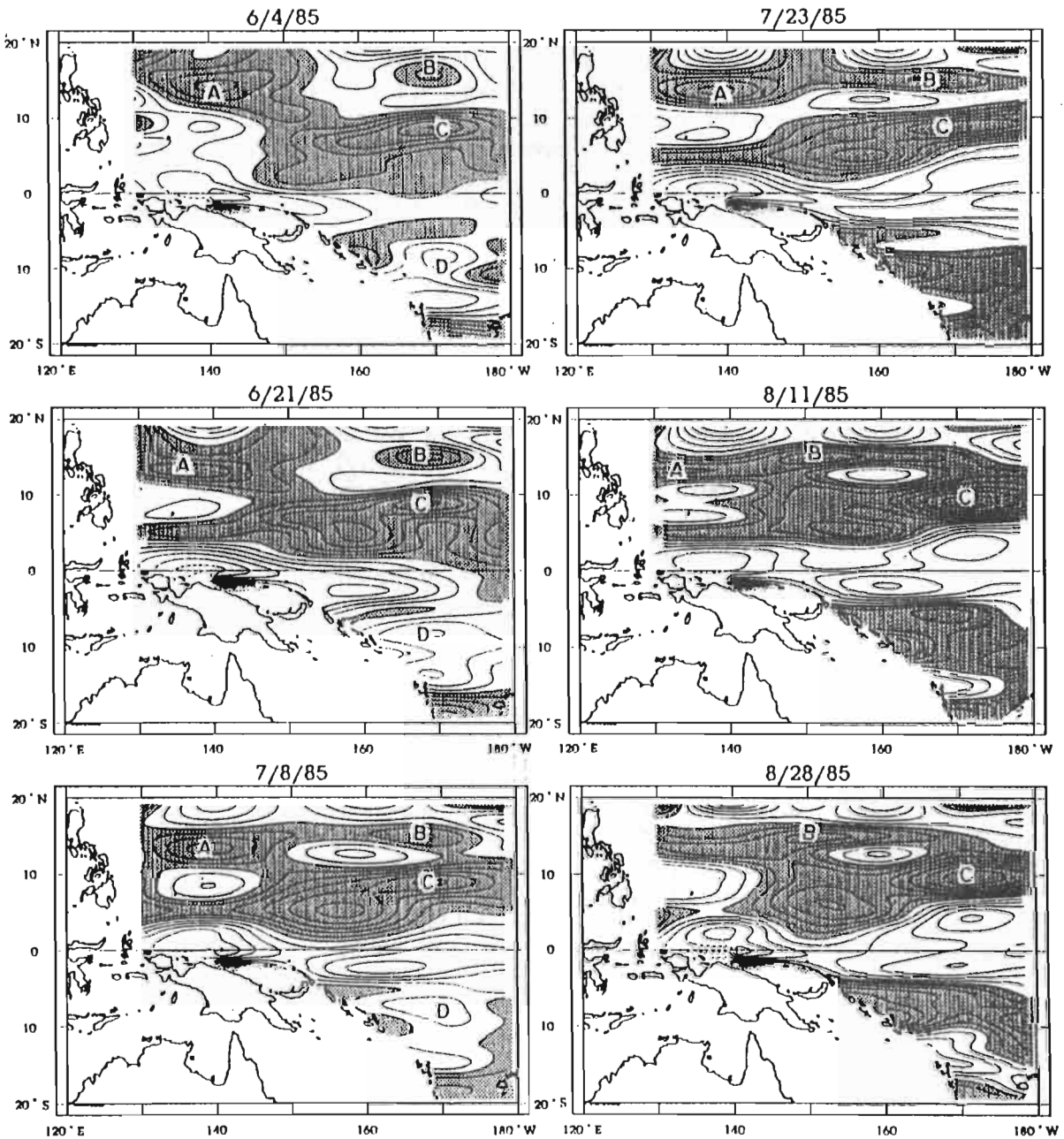


FIG.2. Altimetric sea level maps for June-August 1985. Features evolve smoothly and consistently through this series of maps (CI = 2cm, negative values are shaded).

concentrating on the western tropical Pacific, repeated from Tai et al. (1989). Notice that in the maps the Philippines Archipelago forms the maritime western boundary in the northern hemisphere from the equator to nearly 20°N , while the Solomon Archipelago/New Guinea complex forms the maritime western boundary in the southern hemisphere from the equator to approximately 10°S . Notice too that the sea level residual features labeled alphabetically in Fig.2 can be traced from map to map, often indicating (particularly A and B) westward propagation into the maritime western boundary of the tropical Pacific.

In order to extract the information that this time series of maps of altimetric sea level residuals has concerning the reflection of baroclinic Rossby waves from the maritime western boundary of the tropical Pacific, extended empirical orthogonal function (EEOF) analysis (Graham et al., 1987) was conducted upon the thirty-one 17-day maps of altimetric sea level differences about the mean for the 17-month period represented (i.e., from November, 1985-April, 1987). One EEOF analysis was conducted upon the entire field of altimetric sea level differences from South America to the maritime coast of Asia, allowing the evolution of the basin-scale redistribution of mass to be examined (Fig.4). Then, in order to focus on the reflection activity at the maritime western boundary of the tropical Pacific, the EEOF analysis was repeated upon the western tropical Pacific, from 20°S - 20°N west of 160°W (Fig.5).

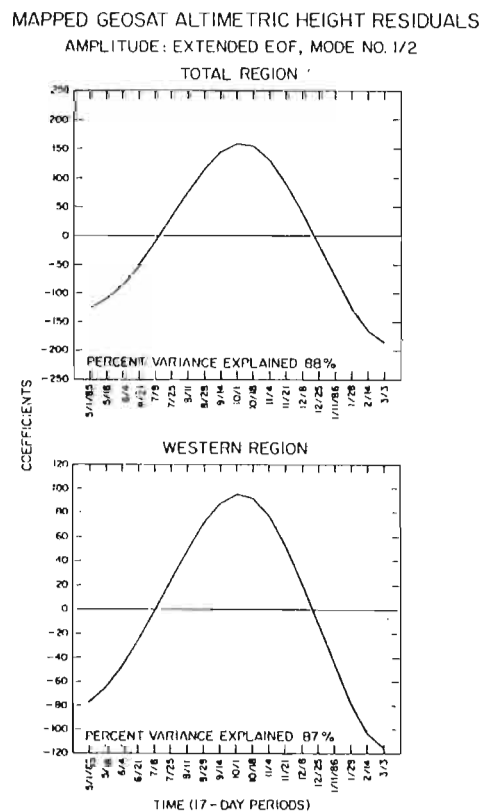


FIG.3. Time sequences for the first extended empirical orthogonal functions of altimetric sea level residual computed for the tropical Pacific (Upper Panel) and the western tropical Pacific (Lower Panel), explaining 88% and 87% of the total variance in the 17-month time sequence. The evolutionary spatial patterns of these functions are given in Figs. 5 and 6.

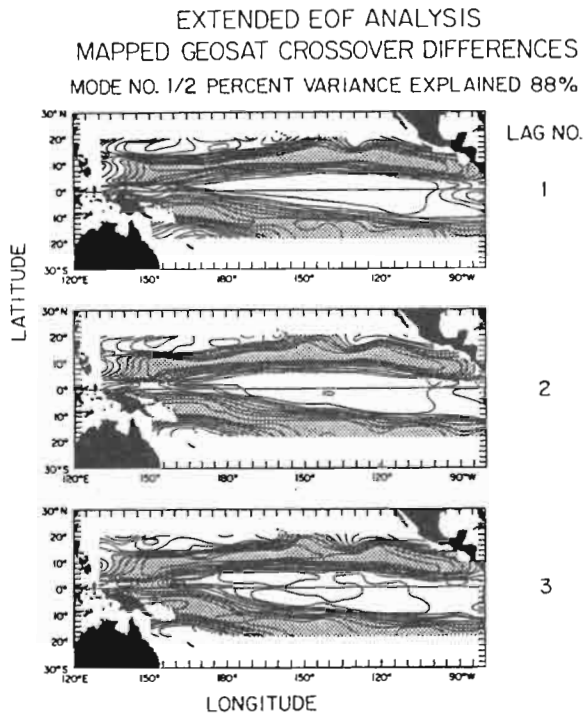


FIG.4.a Time sequence of the first three spatial patterns (1-3) of the first extended empirical orthogonal function for the tropical Pacific, the latter explaining 87% of the total variance in the 17-month time sequence. Shading indicates negative phase.

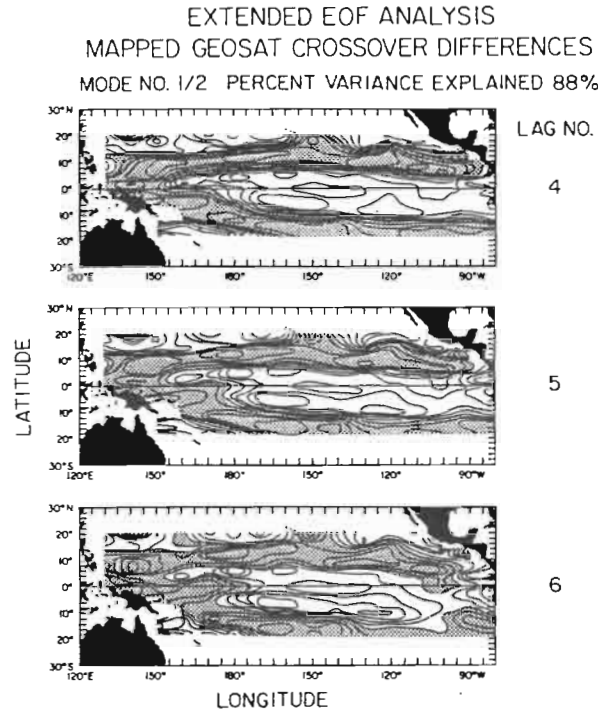


FIG. 4b. Time sequence of the second three spatial patterns (4-6) of the first extended empirical orthogonal function for the tropical Pacific, the latter explaining 87% of the total variance in the 17-month time sequence. Shading indicates negative phase.

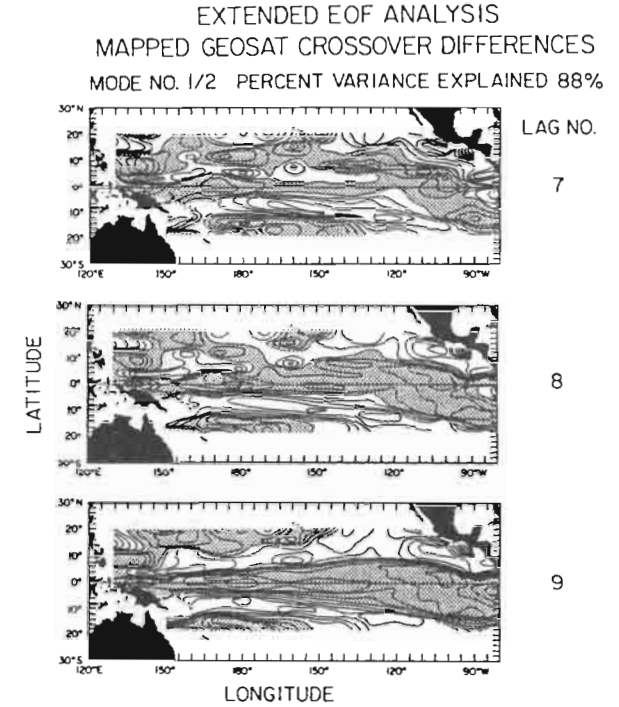


FIG. 4c. Time sequence of the third three spatial patterns (7-9) of the first extended empirical orthogonal function for the tropical Pacific, the latter explaining 87% of the total variance in the 17-month time sequence. Shading indicates negative phase.

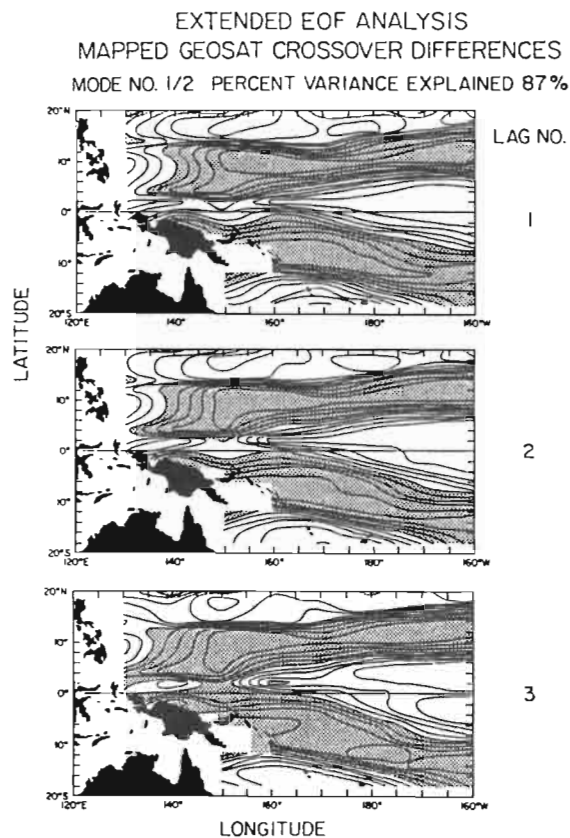


FIG. 5a. Time sequence of the three spatial patterns (1-3) of the first extended empirical orthogonal function for the western tropical Pacific, the latter explaining 88% of the total variance in the 17-month time sequence. Shading indicates negative phase.

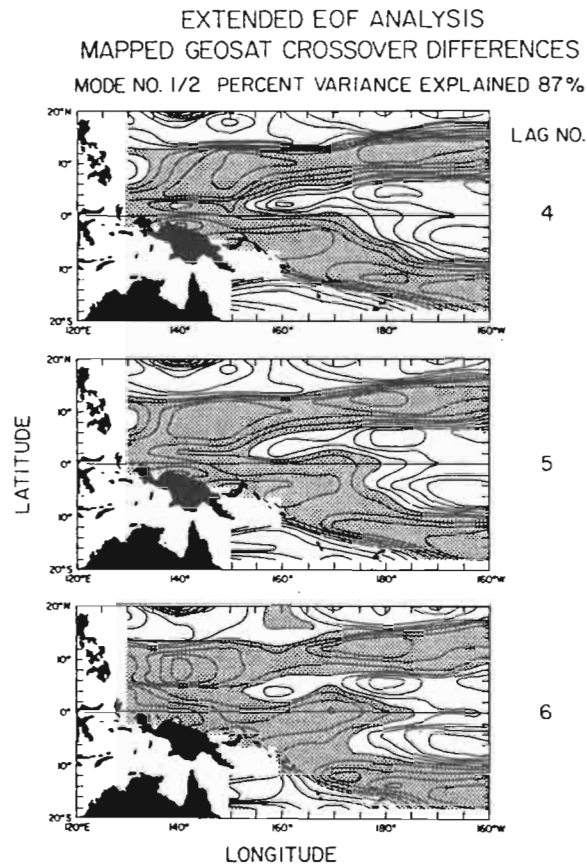


FIG. 5b. Time sequence of the second three spatial patterns (4-6) of the first extended empirical orthogonal function for the western tropical Pacific, the latter explaining 88% of the total variance in the 17-month time sequence. Shading indicates negative phase.

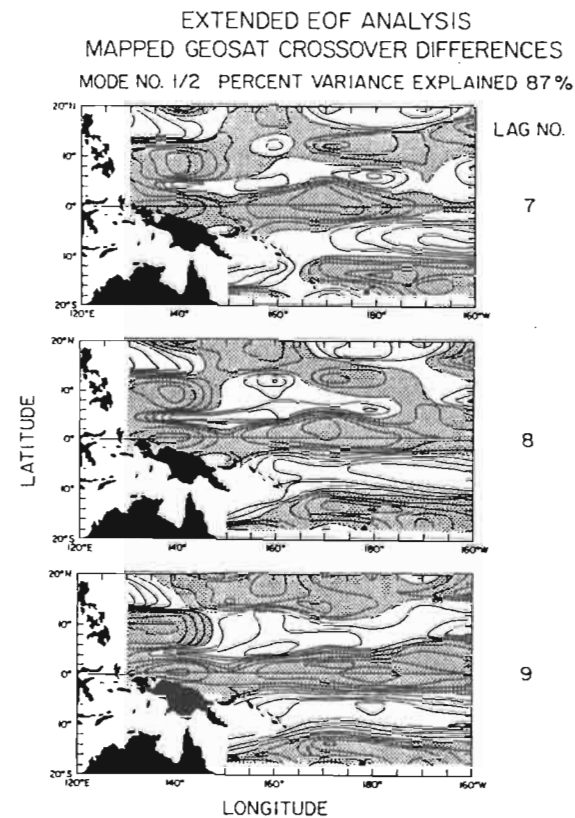


FIG. 5c. Time sequence of the third three spatial pattern (7-9) of the first extended empirical orthogonal function for the western tropical Pacific; the latter explaining 88% of the total variance in the 17-month time sequence. Shading indicates negative phase.

The time sequences of both of these EEOF's is given in Fig.3, with that for the entire tropical Pacific shown in the upper panel, and that for the western Pacific shown in the lower panel. Each are taken from the first two EEOF's, which together account for 88% and 87% of the total variance, respectively, in the tropical Pacific and the western tropical Pacific. The first two EEOF's tend to be redundant and, being orthogonal, give different phases of the same evolutionary behavior in the time sequence of maps (Graham et al., 1987). In this case, the time series of the two analyses are nearly identical, and strongly dominated by the annual cycle.

The EEOF on the basin scale maps is given in Fig. 4a, b, c, showing the evolution of the annual cycle through approximately half a cycle (i.e., 6 months), extending over nine 17-day time periods (i.e., 153 days). The time sequence of nine maps that constitutes the EEOF shows how the spatial pattern in Map 1 evolved into the opposite phase in Map 9 through the spring/autumn transition. In this series of maps, the latitude of approximately 8° marked a boundary where the phase of the annual cycle on the poleward side was opposite that on the equatorward side. This was also found to be true in the complex empirical orthogonal function (CFOF) analysis in Tai et al., (1989). In the present study, by following the evolution of the annual cycle through half a cycle with the aid of the EEOF analysis, from positive residual on the equator (i.e., Map 1) to negative residual on the equator (Map 9), this phase transition from winter to summer (and vice versa) can be understood.

In the first three maps of Fig.4a, the changes that took place in this phase transition are the following. In the off-equatorial region poleward of approximately 8° latitude, the negative residual propagated to the west, evident particularly in the western tropical Pacific. In the western equatorial Pacific, west of 160°E , the negative anomaly began to collapse onto the equator, more from the southern hemisphere north of the Solomon Archipelago/New Guinea complex than from the northern hemisphere. In the northern hemisphere, positive residuals along the coast of the Philippines Archipelago extended southward to the equator in Map 1 and Map 2, where they protruded eastward along the equator; this terminated in Map 3.

In the next three maps (i.e., Maps 4-6 in Fig. 4b), the transition in phase of the annual cycle found negative residuals on the equator in the western Pacific emanating from the Solomon Archipelago/New Guinea complex in the southern hemisphere. Moreover, these negative residuals began to extend eastward along the equator into the eastern equatorial Pacific forming a trough along the equator. In Map 4, this eastward extension of the trough along the equator seems to have originated from the southern hemisphere, but by Map 6 the trough seems to have originated from both hemispheres. At the eastern boundary, an interesting phenomenon began to occur in this sequence of three maps; apparent first-mode equatorial Rossby wave activity appears to have reflected from the eastern boundary (i.e., with local positive maxima at 4°N and 4°S) in response to incident Kelvin wave activity, associated with positive residuals extending northward along the coast of Central America. However, over these three maps (and, as we shall see, over the next three maps) this apparent first-mode equatorial Rossby wave activity did not propagate westward of the Galapagos Archipelago.

In the next three maps (i.e., Maps 7-9 in Fig. 4c), the autumn phase transition from positive to negative sea level residuals along the equator was completed. This occurred with the eastward propagation of negative sea level residuals, initially (Map 7) extending from the west along the equator and confined to the equatorial wave-guide, but later (Map 9) filling the entire region equatorward of approximately 8° latitude, apparently in response to wind stress forcing. In the northern hemisphere western Pacific, negative residuals can be seen to have propagated westward onto the Philippine Archipelago between $5^\circ\text{-}15^\circ\text{N}$, extending equatorward along the maritime western boundary from 15°N to the equator, with negative residuals extending eastward along the

equator from the maritime western boundary of the tropical Pacific. This is indicative of the reflection of incident baroclinic Rossby wave activity and the excitation of baroclinic Kelvin wave activity. In the southern hemisphere western Pacific, positive residuals in the western Pacific began to be found along the Solomon Archipelago, nudging equatorward to begin the process of another phase transition (i.e., this time the spring transition) from the present negative equatorial state to a positive one on the equator.

The EEOF of the western tropical Pacific (i.e., 160°W to the maritime coast of Asia) is given in Fig. 5a, b, c, showing the evolution of the annual cycle through half a cycle (i.e., 6 months), extending over nine 17-day period (i.e. 170 days). It shows in detail the western boundary reflection of the annual baroclinic Rossby wave activity, associated with phase transition of the annual cycle over the entire tropical Pacific shown in Fig. 4a, b, c, and the subsequent Kelvin wave excitation in the equatorial wave-guide.

In the first three maps of Fig. 5a, the changes that took place in the western boundary, associated with the phase transition of the annual cycle from positive to negative residual on the equator, were able to be observed. In the off-equatorial region of the southern hemisphere (i.e., poleward of equatorial wave-guide, the latter extending to approximately 3° latitude), the negative residuals can be seen to have propagated to the west, clearly riding up onto the Solomon Archipelago/New Guinea complex from 160°-150°E, penetrating as far west as 130°E. Over this approximately 1 1/2 month period, the negative residuals also penetrated equatorward and intersected the equator in a relatively broad longitudinal band equatorward of the Solomon Archipelago and New Guinea. Poleward of the equator wave-guide in the northern hemisphere, positive residuals along the coast of the Philippines Archipelago (i.e. from 3°-14°N) extended southward to the equator, where they protruded eastward along the equator, indicative of the excitement of equatorial Kelvin wave activity by the coastal Kelvin-Munk wave activity (Godfrey, 1976). It is important to remember that each altimetric sea level datum along 130°E is a 10° longitude mean, so the information at the longitude extends from 125°-135°, representing information in sea level variability next to the Philippine coast at 123°-127°E, but smearing it with information eastward of there. East of the positive residuals adjacent to the Philippines Archipelago, negative residuals were observed to extend all across the tropical Pacific from 4°-12°N; in Fig. 5a these negative residual can be observed to have propagated to the west over the three maps shown penetrating over the two month period to the maritime western boundary from 2°-6°N and extending toward the equator north of New Guinea.

In the next three maps (i.e. Maps 4-6 in fig. 5b), the transition in annual phase finds the negative residual that had penetrated to the equator north of Solomon Archipelago/New Guinea complex in the western Pacific (over the previous 1 1/2 month) extending eastward along the equator, forming a trough from 130°E-160°W. In Map 4, the eastward extension of this trough along the equator originated from the southern hemisphere, but in Maps 5 and 6 the trough began to originate from both hemispheres, with the contributions from both hemispheres clearly visible. The earlier contribution from the southern hemisphere seemed to have occurred because the maritime western boundary in the southern hemisphere was located 20°-30° of longitude east of that in the northern hemisphere, coupled with the fact that the negative residuals in the off-equatorial region as a whole were relatively symmetric about the equator. The lag of the northern hemisphere behind the southern hemisphere was only 1-2 months. In the last map (i.e., Map 6) of this series of three in Fig. 5b, the off-equatorial negative residuals in the northern hemisphere penetrated to the maritime western boundary at approximately 10°N, with maximum values continuing equatorward along the boundary and extending east along the equator.

In the next three maps (i.e., Maps 7-9 in Fig. 5c) the autumn phase transition in the annual cycle from positive to negative residuals along the equator was completed, with the equatorial wave-guide filled with negative residuals emanating principally from the maritime western boundary in the northern hemisphere from 5-15°N. During these times, the southern hemisphere had positive residuals in the off-equatorial region from 5°-15°S, nudging equatorward to begin the reciprocal process of the spring phase transition from the present negative equatorial state to positive; not so in the northern hemisphere where an intense negative anomaly from 5°-15°N continued to supply off-equatorial influence to the equator via the maritime western boundary, helping to maintain the negative residuals in the equatorial wave-guide. In this maritime western boundary of the northern hemisphere, regional maxima in negative residuals were found directly east of Mindanao near 8°N and east of Halmera near 2°N; smaller values were found in between where a gap occurs in the maritime western boundary. Yet still, indications are that the negative residuals bridged this gap, particularly evident in Maps 6-9 in Fig. 5.

An interesting side-light of this examination of the baroclinic Rossby wave reflection occurring at the maritime western boundary of the tropical Pacific is the reflection (or, rather, the lack thereof) of the incident equatorial kelvin wave activity at the eastern boundary of the tropical Pacific (i.e., South America) that can be seen in Fig. 4a, b, c. The incident annual equatorial baroclinic Kelvin wave was observed to have generated coastal Kelvin wave activity (i.e., traveling poleward) and equatorially trapped Rossby wave activity (i.e., traveling westward). It is observed that the equatorially trapped Rossby wave activity, thus generated, did not propagate westward past the Galapagos Archipelago.

Acknowledgments. We thank Thomas Davis of the Navy Oceanographic Office, who kindly provided us with the GEOSAT crossover differences. Appreciation is given to Ted Walker and Paul Rasmusson who, as programmers, were instrumental in the analysis of these GEOSAT crossover differences. This study was supported principally by NSF Grant OCE86-07962. The research was also supported under NASA's TOPEX Altimetry Research in Ocean Circulation Mission, funded through the Jet Propulsion Laboratory. The computations was done partly on the San Diego Supercomputer Center's CRAY XMP-48.

REFERENCES

- Clarke, A.J., 1989: On the reflection and transmission of low frequency energy at the irregular Pacific Ocean boundary - A preliminary report. In: *Western Pacific International Meeting and Workshop on TOGA-COARE. Noumea, New Caledonia.*
- du Penhoat, Y., and M.A. Cane, 1989: Effect of low latitude western boundary gaps on the reflection of equatorial motions. In: *Western Pacific International Meeting and Workshop on TOGA-COARE. Noumea, New Caledonia.*
- Godfrey, J.S., 1975: On ocean spindown I: A linear experiment. *J. Phys. Oceanogr.*, **5**, 399-459.
- Graham, N., J. Michaelsen, and T.P. Barnett, 1987: An investigation of the El Nino Southern Oscillation cycle with statistical methods. 1. Predictor field characteristics. *J. Geophys. Res.*, **92**, 14, 251-14,270.
- Graham, N., and W.B. White, 1988: The El Nino; a natural oscillator of the Pacific ocean/atmosphere system. *Science*, **240**, 1293-1302.

- Graham, N., T.P. Barnett, V.G. Panchang, O.M. Smedsted, J.J. O'Brien, and R.M. Chervin, 1989: The response of a linear model of the tropical Pacific to surface wind from the NCAR general circulation model. *J. Phys. Oceanogr.*, **19**, 1222-1243
- Meyers, G., 1979: On the annual Rossby wave in the tropical North Pacific Ocean. *J. Phys. Oceanogr.*, **9**, 663-674.
- Pazan, S., and W.B. White, 1987: Short-term climatic variability in the volume budget of the western tropical Pacific during 1979-82. *J. Phys. Oceanogr.*, **17**, 440-454.
- Pazan, S., W.B. White, M. Inoue, and J.J. O'Brien, 1986: Off-equatorial influence in dynamic height upon the equatorial Pacific during the 1982-83 ENSO event. *J. Geophys. Res.*, **91**, 8438-8449.
- Schopf, P.S., and M.J. Suarez, 1988: Vacillations in a coupled ocean-atmosphere model. *J. Atmos. Sci.*, **45**, 549-566.
- Tai, C.K., W.B. White and S.E. Pazan, 1989: GEOSAT crossover analysis in the tropical Pacific 2. Verification analysis of altimetric sea level maps with expendable bathythermograph and island sea level data. *J. Geophys. Res.*, **94**, 897-908.
- White, W.B., 1977: Annual forcing of baroclinic long waves in the tropical North Pacific ocean. *J. Phys. Oceanogr.*, **7**, 50-61.
- White, W.B., 1983: Westward propagation of short-term climate variability in the Western North Pacific Ocean from 1964-1974. *J. Mar. Res.*, **41**, 113-125.
- White, W.B., G. Meyers, J.R. Donguy and S. Pazan, 1985a: Short-term climatic variability of the Pacific ocean during 1979-1982. *J. Phys. Oceanogr.*, **15**, 917-935.
- White, W.B., S. Pazan and B. Li, 1985b: Processes of short-term climatic variability in the baroclinic structure of the interior Western Tropical North Pacific. *J. Phys. Oceanogr.*, **15**, 386-402.
- White, W.B., S. Pazan and M. Inoue, 1987: Hindcast/forecast of ENSO events based upon the redistribution of observed and model heat content in the Western Tropical Pacific. *J. Phys. Oceanogr.*, **17**, 264-280.
- White, W.B., Y.H. He, and S.E. Pazan, 1989: Redistribution of subsurface thermal structure during the onset of the 1982-83 and 1986-87 ENSO events and the 1984-85 anti ENSO event. *J. Phys. Oceanogr.*, (in press).

**WESTERN PACIFIC INTERNATIONAL MEETING
AND WORKSHOP ON TOGA COARE**

Nouméa, New Caledonia

May 24-30, 1989

PROCEEDINGS

edited by

Joël Picaut *

Roger Lukas **

Thierry Delcroix *

* ORSTOM, Nouméa, New Caledonia

** JIMAR, University of Hawaii, U.S.A.

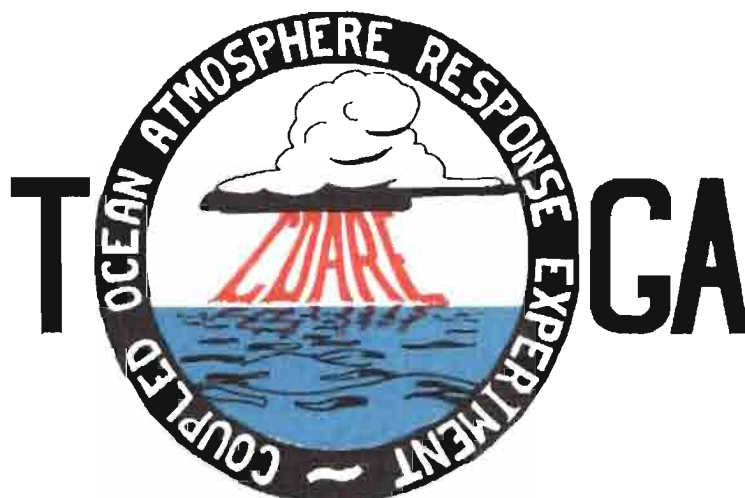


TABLE OF CONTENTS

ABSTRACT	i
RESUME	iii
ACKNOWLEDGMENTS	vi
INTRODUCTION	
1. Motivation	1
2. Structure	2
LIST OF PARTICIPANTS	5
AGENDA	7
WORKSHOP REPORT	
1. Introduction	19
2. Working group discussions, recommendations, and plans	20
a. Air-Sea Fluxes and Boundary Layer Processes	20
b. Regional Scale Atmospheric Circulation and Waves	24
c. Regional Scale Oceanic Circulation and Waves	30
3. Related programs	35
a. NASA Ocean Processes and Satellite Missions	35
b. Tropical Rainfall Measuring Mission	37
c. Typhoon Motion Program	39
d. World Ocean Circulation Experiment	39
4. Presentations on related technology	40
5. National reports	40
6. Meeting of the International Ad Hoc Committee on TOGA COARE	40
APPENDIX: WORKSHOP RELATED PAPERS	
Robert A. Weller and David S. Hosom: Improved Meteorological Measurements from Buoys and Ships for the World Ocean Circulation Experiment	45
Peter H. Hildebrand: Flux Measurement using Aircraft and Radars	57
Walter F. Dabberdt, Hale Cole, K. Gage, W. Ecklund and W.L. Smith: Determination of Boundary-Layer Fluxes with an Integrated Sounding System	81

MEETING COLLECTED PAPERS

WATER MASSES, SEA SURFACE TOPOGRAPHY, AND CIRCULATION

Klaus Wyrtki: Some Thoughts about the West Pacific Warm Pool	99
Jean René Donguy, Gary Meyers, and Eric Lindstrom: Comparison of the Results of two West Pacific Oceanographic Expeditions FOC (1971) and WEPOCS (1985-86)	111
Dunxin Hu, and Maochang Cui: The Western Boundary Current in the Far Western Pacific Ocean	123
Peter Hacker, Eric Firing, Roger Lukas, Philipp L. Richardson, and Curtis A. Collins: Observations of the Low-latitude Western Boundary Circulation in the Pacific during WEPOCS III	135
Stephen P. Murray, John Kindle, Dharma Arief, and Harley Hurlburt: Comparison of Observations and Numerical Model Results in the Indonesian Throughflow Region	145
Christian Henin: Thermohaline Structure Variability along 165°E in the Western Tropical Pacific Ocean (January 1984 - January 1989)	155
David J. Webb, and Brian A. King: Preliminary Results from Charles Darwin Cruise 34A in the Western Equatorial Pacific	165
Warren B. White, Nicholas Graham, and Chang-Kou Tai: Reflection of Annual Rossby Waves at The Maritime Western Boundary of the Tropical Pacific	173
William S. Kessler: Observations of Long Rossby Waves in the Northern Tropical Pacific	185
Eric Firing, and Jiang Songnian: Variable Currents in the Western Pacific Measured During the US/PRC Bilateral Air-Sea Interaction Program and WEPOCS	205
John S. Godfrey, and A. Weaver: Why are there Such Strong Steric Height Gradients off Western Australia ?	215
John M. Toole, R.C. Millard, Z. Wang, and S. Pu: Observations of the Pacific North Equatorial Current Bifurcation at the Philippine Coast	223

EL NINO/SOUTHERN OSCILLATION 1986-87

Gary Meyers, Rick Bailey, Eric Lindstrom, and Helen Phillips: Air/Sea Interaction in the Western Tropical Pacific Ocean during 1982/83 and 1986/87	229
Laury Miller, and Robert Cheney: GEOSAT Observations of Sea Level in the Tropical Pacific and Indian Oceans during the 1986-87 El Nino Event	247
Thierry Delcroix, Gérard Eldin, and Joël Picaut: GEOSAT Sea Level Anomalies in the Western Equatorial Pacific during the 1986-87 El Nino, Elucidated as Equatorial Kelvin and Rossby Waves	259
Gérard Eldin, and Thierry Delcroix: Vertical Thermal Structure Variability along 165°E during the 1986-87 ENSO Event	269
Michael J. McPhaden: On the Relationship between Winds and Upper Ocean Temperature Variability in the Western Equatorial Pacific	283

John S. Godfrey, K. Ridgway, Gary Meyers, and Rick Bailey: Sea Level and Thermal Response to the 1986-87 ENSO Event in the Far Western Pacific	291
Joël Picaut, Bruno Camusat, Thierry Delcroix, Michael J. McPhaden, and Antonio J. Busalacchi: Surface Equatorial Flow Anomalies in the Pacific Ocean during the 1986-87 ENSO using GEOSAT Altimeter Data	301

THEORETICAL AND MODELING STUDIES OF ENSO AND RELATED PROCESSES

Julian P. McCreary, Jr.: An Overview of Coupled Ocean-Atmosphere Models of El Nino and the Southern Oscillation	313
Kensuke Takeuchi: On Warm Rossby Waves and their Relations to ENSO Events	329
Yves du Penhoat, and Mark A. Cane: Effect of Low Latitude Western Boundary Gaps on the Reflection of Equatorial Motions	335
Harley Hurlburt, John Kindle, E. Joseph Metzger, and Alan Wallcraft: Results from a Global Ocean Model in the Western Tropical Pacific	343
John C. Kindle, Harley E. Hurlburt, and E. Joseph Metzger: On the Seasonal and Interannual Variability of the Pacific to Indian Ocean Throughflow	355
Antonio J. Busalacchi, Michael J. McPhaden, Joël Picaut, and Scott Springer: Uncertainties in Tropical Pacific Ocean Simulations: The Seasonal and Interannual Sea Level Response to Three Analyses of the Surface Wind Field	367
Stephen E. Zebiak: Intraseasonal Variability - A Critical Component of ENSO ?	379
Akimasa Sumi: Behavior of Convective Activity over the "Jovian-type" Aqua-Planet Experiments	389
Ka-Ming Lau: Dynamics of Multi-Scale Interactions Relevant to ENSO	397
Pecheng C. Chu and Roland W. Garwood, Jr.: Hydrological Effects on the Air-Ocean Coupled System	407
Sam F. Iacobellis, and Richard C.J. Somerville: A one Dimensional Coupled Air-Sea Model for Diagnostic Studies during TOGA-COARE	419
Allan J. Clarke: On the Reflection and Transmission of Low Frequency Energy at the Irregular Western Pacific Ocean Boundary - a Preliminary Report	423
Roland W. Garwood, Jr., Pecheng C. Chu, Peter Muller, and Niklas Schneider: Equatorial Entrainment Zone : the Diurnal Cycle	435
Peter R. Gent: A New Ocean GCM for Tropical Ocean and ENSO Studies	445
Wasito Hadi, and Nuraini: The Steady State Response of Indonesian Sea to a Steady Wind Field	451
Pedro Ripa: Instability Conditions and Energetics in the Equatorial Pacific	457
Lewis M. Rothstein: Mixed Layer Modelling in the Western Equatorial Pacific Ocean	465
Neville R. Smith: An Oceanic Subsurface Thermal Analysis Scheme with Objective Quality Control	475
Duane E. Stevens, Qi Hu, Graeme Stephens, and David Randall: The hydrological Cycle of the Intraseasonal Oscillation	485
Peter J. Webster, Hai-Ru Chang, and Chidong Zhang: Transmission Characteristics of the Dynamic Response to Episodic Forcing in the Warm Pool Regions of the Tropical Oceans	493

MOMENTUM, HEAT, AND MOISTURE FLUXES BETWEEN ATMOSPHERE AND OCEAN

W. Timothy Liu: An Overview of Bulk Parametrization and Remote Sensing of Latent Heat Flux in the Tropical Ocean	513
E. Frank Bradley, Peter A. Coppin, and John S. Godfrey: Measurements of Heat and Moisture Fluxes from the Western Tropical Pacific Ocean	523
Richard W. Reynolds, and Ants Leetmaa: Evaluation of NMC's Operational Surface Fluxes in the Tropical Pacific	535
Stanley P. Hayes, Michael J. McPhaden, John M. Wallace, and Joël Picaut: The Influence of Sea-Surface Temperature on Surface Wind in the Equatorial Pacific Ocean	543
T.D. Keenan, and Richard E. Carbone: A Preliminary Morphology of Precipitation Systems In Tropical Northern Australia	549
Phillip A. Arkin: Estimation of Large-Scale Oceanic Rainfall for TOGA	561
Catherine Gautier, and Robert Frouin: Surface Radiation Processes in the Tropical Pacific	571
Thierry Delcroix, and Christian Henin: Mechanisms of Subsurface Thermal Structure and Sea Surface Thermo-Haline Variabilities in the South Western Tropical Pacific during 1979-85 - A Preliminary Report	581
Greg. J. Holland, T.D. Keenan, and M.J. Manton: Observations from the Maritime Continent : Darwin, Australia	591
Roger Lukas: Observations of Air-Sea Interactions in the Western Pacific Warm Pool during WEPOCS	599
M. Nunez, and K. Michael: Satellite Derivation of Ocean-Atmosphere Heat Fluxes in a Tropical Environment	611

EMPIRICAL STUDIES OF ENSO AND SHORT-TERM CLIMATE VARIABILITY

Klaus M. Weickmann: Convection and Circulation Anomalies over the Oceanic Warm Pool during 1981-1982	623
Claire Perigaud: Instability Waves in the Tropical Pacific Observed with GEOSAT	637
Ryuichi Kawamura: Intraseasonal and Interannual Modes of Atmosphere-Ocean System Over the Tropical Western Pacific	649
David Gutzler, and Tamara M. Wood: Observed Structure of Convective Anomalies	659
Siri Jodha Khalsa: Remote Sensing of Atmospheric Thermodynamics in the Tropics	665
Bingrong Xu: Some Features of the Western Tropical Pacific: Surface Wind Field and its Influence on the Upper Ocean Thermal Structure	677
Bret A. Mullan: Influence of Southern Oscillation on New Zealand Weather	687
Kenneth S. Gage, Ben Basley, Warner Ecklund, D.A. Carter, and John R. McAfee: Wind Profiler Related Research in the Tropical Pacific	699
John Joseph Bates: Signature of a West Wind Convective Event in SSM/I Data	711
David S. Gutzler: Seasonal and Interannual Variability of the Madden-Julian Oscillation	723
Marie-Hélène Radenac: Fine Structure Variability in the Equatorial Western Pacific Ocean	735
George C. Reid, Kenneth S. Gage, and John R. McAfee: The Climatology of the Western Tropical Pacific: Analysis of the Radiosonde Data Base	741

Chung-Hsiung Sui, and Ka-Ming Lau: Multi-Scale Processes in the Equatorial Western Pacific	747
Stephen E. Zebiak: Diagnostic Studies of Pacific Surface Winds	757

MISCELLANEOUS

Rick J. Bailey, Helene E. Phillips, and Gary Meyers: Relevance to TOGA of Systematic XBT Errors	775
Jean Blanchot, Robert Le Borgne, Aubert Le Bouteiller, and Martine Rodier: ENSO Events and Consequences on Nutrient, Planktonic Biomass, and Production in the Western Tropical Pacific Ocean	785
Yves Dandonneau: Abnormal Bloom of Phytoplankton around 10°N in the Western Pacific during the 1982-83 ENSO	791
Cécile Dupouy: Sea Surface Chlorophyll Concentration in the South Western Tropical Pacific, as seen from NIMBUS Coastal Zone Color Scanner from 1979 to 1984 (New Caledonia and Vanuatu)	803
Michael Szabados, and Darren Wright: Field Evaluation of Real-Time XBT Systems	811
Pierre Rual: For a Better XBT Bathy-Message: Onboard Quality Control, plus a New Data Reduction Method	823